Ion broadening of Ar I lines in a plasma

Douglas W. Jones, W. L. Wiese, and L. A. Woltz
Atomic and Plasma Radiation Division, National Bureau of Standards, Gaithersburg, Maryland 20899
(Received 17 January 1986)

We have measured the profiles of plasma-broadened, slightly red-shifted spectral lines of neutral argon with a wall-stabilized arc and performed a detailed line-shape analysis with a computerized data acquisition and processing system. According to Stark broadening theory, isolated lines of neutral atoms in dense plasmas are broadened mostly by electron impact, which results in symmetric Lorentzian profiles. An additional small broadening contribution, which is asymmetric in nature, is due to the plasma ions. This difference in symmetries provides the possibility of separating ion broadening effects from the electron broadening. In full agreement with the quasistatic theory of ion broadening, our experiment shows asymmetry patterns with characteristic minima and maxima near the central part of the lines. While the positions of these extrema—as well as the zero crossing point—stay essentially constant for all lines when compared on a reduced wavelength scale, the amplitudes of the extrema vary from line to line. Measurements of the amplitudes thus allow, by comparison with theoretical asymmetry patterns, the determination of ion broadening parameters.

I. INTRODUCTION

According to Stark broadening theory,[1] isolated spectral lines of neutral atoms other than hydrogen are mostly broadened by electron impact in dense plasmas. This electron-impact broadening leads to a *symmetrical* line profile of Lorentzian shape. A much smaller additional contribution to the line broadening arises from the plasma ions and is *asymmetrical* in nature. Exploiting this difference in symmetries, we have developed an experimental technique[2] to isolate the asymmetries caused by ion broadening. While these asymmetries are quite small, precise measurements are possible with the assistance of computerized data-acquisition systems and the utilization of quiescent steady-state plasma sources. Recently, we investigated the asymmetry patterns of plasma broadened C I lines[2] by end-on observations of a wall-stabilized arc operated with CO_2-Ar mixtures, and obtained the following principal results.

(a) The asymmetry patterns of various C I lines (we observed 11 lines of the $3s$-$4p$ array) appear remarkably similar having maxima, minima, and nodes of deviations from symmetrical Lorentzian shapes all at the same reduced wavelength positions.

(b) The only apparent variations in the asymmetry patterns of various lines are their amplitudes, which we found to be directly related to their calculated ion-broadening parameters.

(c) The very close agreement with theoretical asymmetry patterns strongly supports the prediction by the quasistatic theory of ion broadening[1] of a universal reduced line shape which depends only on two parameters: the ion broadening parameter A and the Debye screening parameter R.

Our study of C I lines was, however, confined to only one transition array ($3s$-$4p$). Furthermore, few of the lines were well "isolated;" most lines had another line of significant strength in their spectral vicinity, either from carbon or argon. For our plasma conditions, the triplet lines were located within a few half-widths of each other, and in one case within one half-width [the half-width is always defined here as the *full* width at half maximum intensity (FWHM)]. In such cases of spectrally overlapping lines, the uncertainties in extracting the asymmetry patterns became quite large for the region several FHWM's away from the line centers. Thus, it was difficult to determine precisely the true shapes of these lines far from their line centers. It seems therefore desirable to broaden the experimental knowledge of ion broadening effects, (a) by studying lines of other chemical elements, (b) by finding spectral lines which are well isolated from other lines so that no corrections for the influence of neighboring lines have to be applied, and (c) by finding conditions of optimum plasma source stability in order to obtain minimal noise in the data.

The element which best fulfills conditions (b) and (c) is argon, and it is therefore chosen as the subject of this study. Stabilized arcs operating in argon exhibit excellent stability, and several of the prominent $4s$-$5p$ Ar I lines are sufficiently well spaced from other lines to serve as isolated lines.

II. INSTRUMENTATION AND EXPERIMENTAL METHOD

Since we have recently described our laboratory setup and the measurement procedures in detail,[2,3] including the critically important computerized data-acquisition and analysis system, it suffices here to provide only a summary listing of the principal experimental factors.

(a) Plasma source. The emission source used in these studies was a wall-stabilized arc of 4.2 mm diameter operated at currents of 40 and 45 A. For the end-on observations of Ar I lines, we operated the midsection of the arc in a slow flow of argon gas with a small admixture of hydrogen (typically about 1 vol. %) for H_β Stark-width

diagnostics. In a few runs we used pure argon in the mid-section at otherwise identical conditions to avoid interference from overlapping hydrogen lines. The end sections of the arc, including the electrode areas, were always operated in helium to minimize thermal gradients in the argon plasma which would distort the Ar I line profiles.

(b) Spectrometer. We used a 2.25-m Czerny-Turner monochromator with a 1800-lines/mm holographic grating, and 22.5-μm entrance and exit slits, which produced an instrument width (FWHM) of about 0.05 Å. A cooled photomultiplier tube with a GaAs photocathode was used as the detector. Spectra were scanned by this system in a stepwise fashion that was precisely controlled by the data-acquisition computer.

(c) Data acquisition. Up to 200 data points were accumulated per line profile by the data-acquisition computer which sampled the photoelectric signal 500 times at 0.01 s intervals for each data point. Dark current and spectral sensitivity were routinely monitored to correct for any variations over the range of a line profile.

(d) Self-absorption checks. A concave mirror behind the arc focused the source back into itself. A constant proportionality factor was obtained for the signals from the arc, relative to the signals from the arc plus its image, at all wavelengths across the investigated line shapes and indicated the absence of measurable self-absorption effects in this study.

(e) Plasma analysis. Measurements of the width of the hydrogen line H_β yielded the electron density via the well-established Vidal-Cooper-Smith (VCS) Stark broadening theory.[4] The temperature was then determined via the equilibrium and conservation equations for local-thermodynamic-equilibrium (LTE) plasmas.[5] The numerical results for the two applied arc currents are listed at the bottom of Table I.

III. THEORETICAL CONSIDERATIONS

In 1962, Griem, Baranger, Kolb, and Oertel[6] developed a general theory for the broadening of nonhydrogenic lines in plasmas, which they applied to helium and which Griem[7] subsequently extended to other elements. In this theory, the broadening due to electron collisions is treated by an impact approximation. For the ions, the following two cases are treated: (a) when the motion of the ions can be neglected, the quasistatic approximation is used, which is corrected for ion-ion correlations and Debye shielding; and (b) when the time dependence of the ion microfields cannot be neglected, ion-dynamical corrections are included. The calculations show that electron-impact broadening is usually dominant and ion broadening contributes typically only 10—20 % to the total linewidths and somewhat more to the shifts. Electron-impact broadening yields a shifted but symmetric profile of Lorentzian shape, while the ion contributions introduce both asymmetries and an additional shift. (Both shifts are in the vast majority of cases red shifts, as is the case for all lines investigated here.) This fundamental difference in symmetries provides the possibility of isolating experimentally the asymmetric part due to the ion contribution.

For the quasistatic ion case, line profiles are obtained by averaging electron-impact profiles over the static shifts due to the instantaneous ion fields, using a suitable distribution function for the microfield strength. On a reduced frequency scale, Griem's final result for the line profile is[1,6,7]

$$j_{A,R}(x)=\frac{1}{\pi}\int_0^\infty d\beta\, W_R(\beta)/[1+(x-A^{4/3}\beta^2)^2]\,, \qquad (1)$$

where x is a reduced frequency, which is given by $x=2(\omega-\omega_0-d)/w_e$, with ω the frequency, ω_0 the center frequency of the unperturbed line, d the shift due to elec-

TABLE I. Comparison of measured and theoretical total line widths (FWHM) for the nine transitions and two plasma conditions of this study. Measured widths have been corrected for instrument and Doppler broadening, which are about 0.005 nm and 0.006 nm, respectively. The uncertainty in the total widths is ~5%. Tests for the validity of the quasistatic approximation of ion broadening were carried out using the measured widths and calculating σ of Eq. (5); all σ values are substantially greater than unity indicating that this approximation is valid.

Transition	Wavelength (nm)	FWHM (nm) Expt.	Theory	σ [Eq. (5)]	FWHM (nm) Expt.	Theory	σ [Eq. (5)]
$4s'[\frac{1}{2}]^\circ_0$-$5p[\frac{1}{2}]_1$	452.23	0.120		2.4	0.134		2.3
$4s'[\frac{1}{2}]^\circ_1$-$5p'[\frac{1}{2}]_0$	425.94	0.144	0.186	3.3			
$4s'[\frac{1}{2}]^\circ_1$-$5p[\frac{1}{2}]_0$	451.07	0.157	0.250	3.2	0.179	0.281	3.5
$4s'[\frac{1}{2}]^\circ_1$-$5p[\frac{1}{2}]_1$	470.23	0.132		2.5	0.150		2.7
$4s'[\frac{1}{2}]^\circ_1$-$5p[\frac{3}{2}]_1$	459.61	0.139		2.7	0.150		3.0
$4s'[\frac{1}{2}]^\circ_1$-$5p[\frac{5}{2}]_2$	462.84	0.136		2.6	0.151		2.8
$4s[\frac{3}{2}]^\circ_1$-$5p[\frac{3}{2}]_1$	427.22	0.118	0.139	2.7			
$4s[\frac{3}{2}]^\circ_1$-$5p[\frac{5}{2}]_2$	430.01	0.117		2.6			
$4s[\frac{3}{2}]^\circ_2$-$5p[\frac{3}{2}]_2$	415.86	0.121		2.9			
Temperature:		11 878 K			12 087 K		
Electron density:		6.21×10^{16} cm^{-3}			6.98×10^{16} cm^{-3}		

tron impact, and w_e the electron-impact width (FWHM). A is the ion broadening parameter, and $W_R(\beta)$ is the microfield strength distribution function for a normalized field strength $\beta=F/F_0$, with F_0 being the Holtsmark field strength.[1,6] For the distribution function the results of Hooper's calculations[8] are used, which include ion-ion correlations and Debye shielding by electrons. This distribution function is parametrized by the Debye shielding parameter R, which is defined as the ratio of mean inter-ion distance ρ_m to the Debye radius ρ_D,

$$R=\rho_m/\rho_D=6^{1/3}\pi^{1/6}eN_e^{1/6}(kT)^{-1/2}, \tag{2}$$

where N_e is the electron density and T the temperature of the plasma, and where the plasma is assumed to consist of neutral and singly ionized atomic species and electrons only.

In the above result for the line shape, the small dependence of the static quadratic Stark splitting on the magnetic quantum numbers is neglected, i.e., the splitting into levels with different m by the ion field is assumed to be so small that it is ignored.

The criterion given by Griem[1] for the validity of the quasistatic approximation is based upon the consideration that the frequencies characterizing the ion fields should be considerably smaller than the characteristic frequency for the electron-impact broadening, which corresponds to the electron-impact width $w_e/2$ (FWHM). The characteristic frequency for collisions of ions, moving with relative velocities v_r and having a mean inter-ion separation $\rho_m=(4\pi N_e/3)^{-1/3}$, is v_r/ρ_m. Thus the condition

$$\sigma=\frac{w_e\rho_m}{2v_r}>1 \tag{3}$$

is required for the validity of the quasistatic approximation.

Substituting $v_r=(8kT/\pi\mu)^{1/2}$, where μ is the reduced mass of the radiator-ion perturber system, one obtains, for singly ionized plasmas,

$$\sigma=\frac{w_e(4\pi N_e/3)^{-1/3}}{(32kT/\pi\mu)^{1/2}}>1\,. \tag{4}$$

In numerical form, this is

$$\sigma=(4.015\times10^{14})(\mu/T)^{1/2}N_e^{-1/3}(w_e/\lambda_0^2)>1\,, \tag{5}$$

where μ is in amu, T is in K, N_e is in cm^{-3}, and w_e and λ_0 are in Å. In order to test this criterion on an observed line it is acceptable to substitute the measured linewidth for the electron-impact width, because the measured width (which includes the ion broadening contributions) is typically only slightly larger than the corresponding electron-impact width. Many comparisons with Griem's semiclassical theory have shown that this is true for visible lines emitted by neutral species in LTE plasmas. (For our experimental conditions, other contributions to the linewidth—Doppler, van der Waals, and instrumental broadening—are calculated to be negligibly small when folded into the combined Voigt-type profile,[9] since—*per se*—they would amount at most to about 2% of the observed width.)

Table I contains values of σ obtained in this manner for the Ar I lines investigated, and a comparison of calculated[1] and observed total widths. It is seen that for all investigated lines the validity criterion for the quasistatic approximation is satisfied for the conditions of our plasma. [The above criterion of Eq. (3) is mutually exclusive with the inequality $\sigma A^{1/3}<1$ given by Barnard *et al.*[10] as a condition for the application of their ion dynamic theory. The ion broadening parameters A for the Ar I lines investigated in this study have values greater than 0.08 and σ always exceeds 2.3, yielding $\sigma A^{1/3}>1$, so that the application of their more complex ion dynamic theory is not required.] The measured line shape data thus may be compared with theoretical line profiles[1,11] calculated for the quasistatic ion regime.

IV. ANALYSIS OF OBSERVED AND CALCULATED LINE PROFILES

In order to isolate the asymmetries caused by ion broadening we performed least-squares fits of the measured (and calculated) line profiles to symmetrical Lorentzian curves which rest on a smooth continuum background simulated by a cubic polynomial. The polynomial allows for a slight curvature in the background which can be caused by the wings of strongly broadened nearby lines. Since our procedure gives the best possible match between the fitted curve and the input data by simultaneously optimizing the seven free parameters of the fitted spectra (three for the Lorentzian and four for the continuum), the deviations from the fitted curves are determined in a straightforward manner.

The normalized deviation $\Delta(\delta\lambda)$ of a data point from the corresponding fitted Lorentzian at a wavelength distance $\delta\lambda=\lambda-\lambda_0$ from the Lorentzian center wavelength λ_0 may be expressed as

$$\Delta(\delta\lambda)=\frac{I(\lambda_0+\delta\lambda)-L(\lambda_0+\delta\lambda)}{L(\lambda_0)}\,, \tag{6}$$

where $I(\lambda)$ is the observed spectral radiance profile and $L(\lambda)$ is the least-squares-fit Lorentzian. The antisymmetric nature of the deviations we have observed makes the antisymmetric deviation function

$$\Delta_a(\delta\lambda)=\tfrac{1}{2}[\Delta(\delta\lambda)-\Delta(-\delta\lambda)] \tag{7}$$

of particular interest in determining ion broadening parameters, since our previous work[2] suggests a simple, direct relationship between the amplitude of these antisymmetrical deviations and values of A.

For consistency, the experimental and theoretical $j_{A,R}(x)$ profiles were subjected to the same analysis. We also did this in our previous study of C I lines,[2] but encountered problems due to the limited scope of the numerical tabulations[1] of theoretical Stark profiles. The coarse spacing of the data points and the early cutoffs in the line wings at -1 FWHM and $+2.5$ FWHM made detailed quantitative comparisons difficult and imprecise. Extension of the tabulated profiles with asymptotic wing formulas given by Griem[1] for large x, i.e.,

$$j(x)\approx\begin{cases}\dfrac{1}{\pi x^2}[1+A(3\pi/4)x^{1/4}] \quad \text{for } x>0 & \text{(8a)}\\ \dfrac{1}{\pi x^2} \quad \text{for } x<0\,, & \text{(8b)}\end{cases}$$

also proved to be too imprecise to be useful in alleviating these problems.

Therefore, one of us (L.A.W.) undertook new line-profile calculations based on Eq. (1) using the field strength distribution functions of Hooper.[8] Stark profiles were calculated over the extended wavelength range $\pm 5w_e$ from line center with a dense point spacing. (Points which coincide with Griem's earlier calculation agree with those results to three significant figures.) A tabulation of these results for a range of R and A values will be published elsewhere.[11] All comparisons of measured and calculated profiles have been made with these new theoretical profiles.

Antisymmetric deviation functions for the calculated line profiles were generated by performing again a least-squares fit to Lorentzian profiles on a smooth continuum background represented by a cubic polynomial, completely analogous to the analysis of the experimental line profiles. Although the theoretical line profiles have no continuum background pedestal, this portion of the least-squares fitting procedure was left intact in order to achieve identical analyses of the theoretical and measured line-profile data. The continuum background contribution to the synthetic spectra resulting from the theoretical profiles was always extremely small and, in fact, may be considered to be essentially zero to within the accuracy of the fitting procedure itself. Equations (6) and (7) were then applied to these results to yield the family of antisymmetric deviation functions shown in Fig. 1. Since the wavelength intervals from the line center are given in units of the FWHM of the fitted Lorentzians generated by the least-squares procedure, the wavelength offset positions for the various line profiles are scaled according to the width of the corresponding best-fit Lorentzian. The positions and amplitudes of the characteristic features of these curves are summarized in Table II. The nearly constant positions of the minima, zero-crossing node, and maxima despite a 20-fold increase in A values is most striking. The residual variations in the values shown in Table II may well be merely an artifact of the fitting procedures. The data in Table II also indicate an almost linear relationship between the ion broadening parameter A and the amplitudes of both the minima and the maxima for these theoretical profiles. The specific relationship between the amplitude of the *minimum* and the value of A may be utilized for accurate experimental determina-

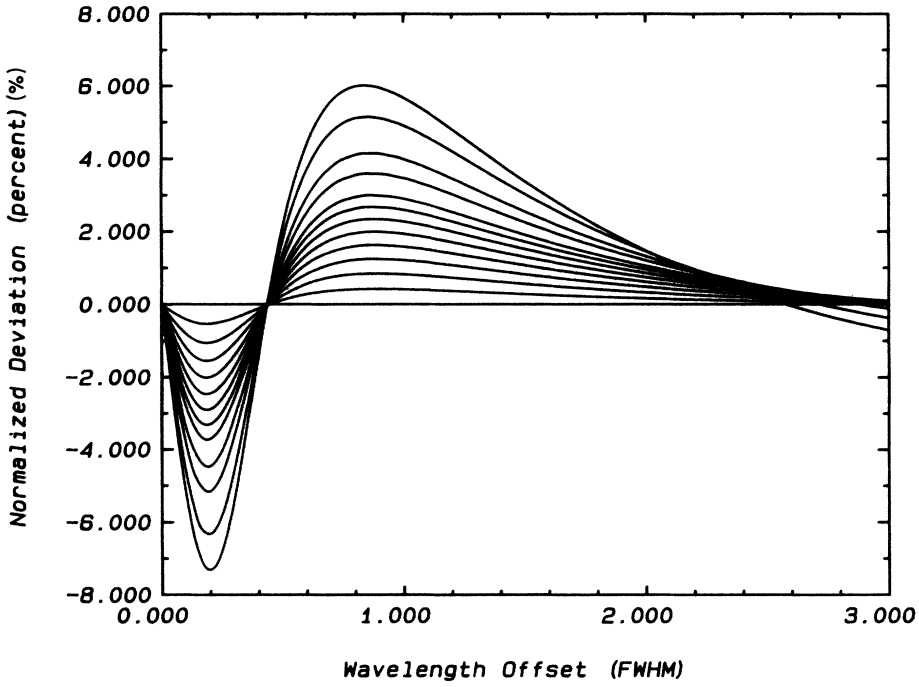

FIG. 1. Calculated antisymmetric deviation functions for values of the ion broadening parameter A ranging from 0.025 to 0.500 and a Debye shielding parameter R of 0.55. The curves plot the results of Eq. (7) when the new line-profile calculations based on Eq. (1) are subjected to the same analysis as the measured line profiles. In order of increasing deviation amplitude the curves correspond to A values of 0.025, 0.050, 0.075, 0.100, 0.125, 0.150, 0.175, 0.200, 0.250, 0.300, 0.400, and 0.500, respectively. The wavelength offset scale is given in units of the FWHM of the least-squares-fitted Lorentzian corresponding to each calculated profile. The apparent decrease to negative values near wavelength offsets of 3 FWHM for the curves with the largest values of A is an artifact of the analysis procedure caused by the finite wavelength range of the digital line profiles and the extremely non-Lorentzian shape of these highly distorted profiles.

TABLE II. Theoretical asymmetry data. Positions and amplitudes of the characteristic features of the antisymmetric deviation functions obtained by subjecting the calculated line profiles of Ref. 11 to the same analysis as the measured line-profile data (details in the text). The value of the Debye shielding parameter R is 0.55 for all calculated profiles. The position of the minima, zero-crossing nodes, and maxima are all given in units of the FWHM of the least-squares-fitted Lorentzian for the corresponding calculated line profile. The amplitudes of the normalized deviations follow from Eqs. (6) and (7) and are given in percent.

Ion broadening parameter	Positions as functions of the FWHM			Amplitudes of minimum and maximum deviations	
A	Minimum	Node	Maximum	Min. (%)	Max. (%)
0.025	0.188	0.451	0.886	−0.53	0.43
0.050	0.187	0.444	0.872	−1.05	0.85
0.075	0.187	0.443	0.877	−1.54	1.25
0.100	0.186	0.442	0.879	−2.01	1.63
0.125	0.186	0.441	0.880	−2.47	2.00
0.150	0.186	0.441	0.874	−2.91	2.34
0.175	0.186	0.440	0.863	−3.32	2.67
0.200	0.186	0.439	0.859	−3.73	2.99
0.250	0.190	0.439	0.849	−4.48	3.59
0.300	0.192	0.437	0.861	−5.17	4.14
0.400	0.194	0.437	0.855	−6.33	5.14
0.500	0.196	0.436	0.836	−7.32	6.01

tions of A, because in this region of a measured line profile the signal-to-noise ratio is optimal and the effects of nearby lines are minimal.

V. RESULTS AND DISCUSSION

The principal objective of this study was the analysis of asymmetries resulting from ion broadening effects for isolated spectral lines having minimal overlap with neighboring lines for conditions of optimum plasma source stability. The nine, all slightly red-shifted lines of the Ar I $4s$-$5p$ transition array investigated in this study satisfy these conditions quite well; these lines are at 415.86, 425.94, 427.22, 430.01, 451.07. 452.23, 459.61, 462.84, and 470.23 nm. Measured line profiles for these nine lines were analyzed in terms of the deviation functions described above for the theoretical profiles, and the antisymmetric deviation results for several scans of each line were averaged together to reduce the effects of random noise. The measured antisymmetric deviation curves for the nine lines of this study clustered into three distinct groups of curves with varying amplitudes, but essentially identical shapes. One representative data curve from each of these three groups was chosen for display in Fig. 2, in which these measured data are compared with three of the theoretical curves from Fig. 1. No attempt has been made to "fit" the theoretical curves to the experimental data curves. Instead, the three theoretical curves from Fig. 1 which span the range of the measured antisymmetric deviations in the vicinity of the minimum are merely reproduced in Fig. 2. Coincidentally, however, the theoretical curve corresponding to an ion-broadening parameter of 0.150 overlaps the measured deviation curve for the line at 451.07 nm almost perfectly from a wavelength offset of about 0.6 FWHM to the line center at 0.0 FWHM. This excellent agreement appears to indicate that the calculated asymmetries which follow from the quasistatic ion approximation embedded in Eq. (1) are quite accurate, with no discernible discrepancies in this wavelength region.

Thus it is not clear if the disagreements between theory and experiment beginning near the maxima in Fig. 2 and extending to larger wavelength distances from line center are a real effect or an artifact of the measurement and analysis procedures. For larger wavelength distances from the line center, the measured data suffer from decreasing signal levels which degrade the signal-to-noise ratio, making the data less reliable. Also, the ratio of spectral line radiance to continuum background radiance is much decreased, making the accuracy of the continuum background determination much more critical.

The positions and amplitudes of the characteristic features of the antisymmetric deviation functions obtained from the measured line profiles are summarized in Table III for all nine lines investigated in this study. It is seen that the positions of the minima, zero-crossing nodes, and maxima are essentially constant, with average values and corresponding standard deviations indicated at the bottom of the table. Comparison of these averages with corresponding data for the theoretical profiles from Table II (the case for $A=0.125$ is again listed as the last line of Table III) shows overall agreement within 10% for the positions of the extrema and the node. The last two columns of Table III provide data on the ion broadening parameter A. The measured values of A are obtained from the empirical relationship between A and the amplitude of the minimum (M) shown in the first and fifth columns of Table II (and discussed earlier) and are estimated to have an uncertainty of about 10%. The theoretical values of A shown in the last column of Table III are obtained, appropriately scaled, from the tables of Griem,[1] who computed numerical A values with a quantum-mechanical approach.

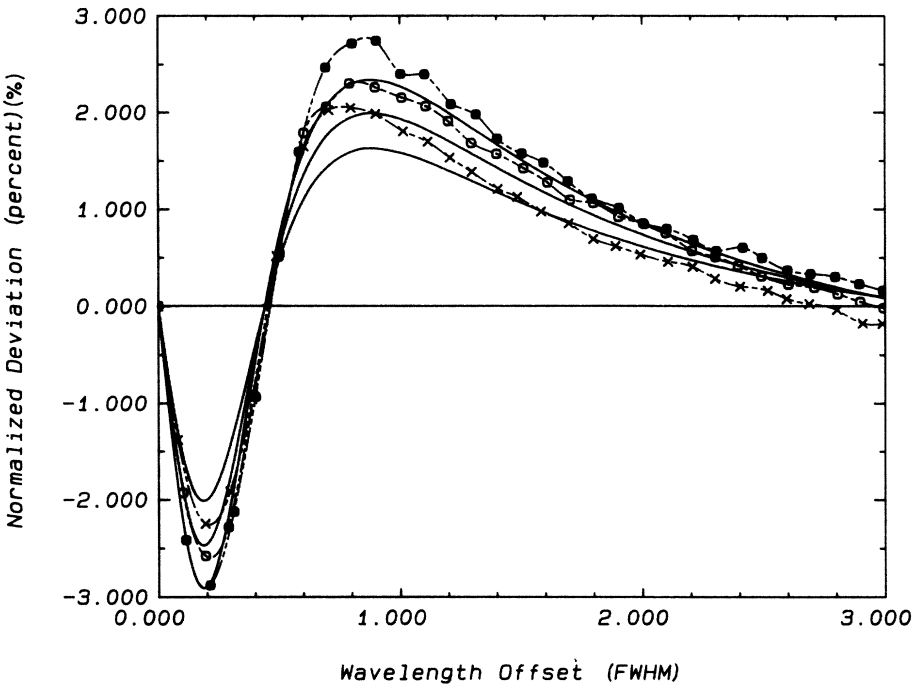

FIG. 2. Comparison plot of the antisymmetric deviation functions for three representative measured line profiles and the three closest theoretical results from Fig. 1. The three theoretical curves are the solid lines and correspond, in order of increasing amplitude, to ion broadening parameters of 0.100, 0.125, and 0.150, respectively. The curves for the measured line profiles are the dashed lines marked by symbols. The curve marked with solid squares displays the antisymmetric deviation measurements for the Ar I $4s$-$5p$ transition at 451.07 nm, while the one marked with open squares corresponds to the 427.22-nm transition and the one marked with crosses corresponds to the 425.94 nm transition of this array. Values of the ion broadening parameter for the three measured profiles shown here are 0.151 for the 451.07-nm line, 0.133 for the 427.22-nm line, and 0.114 for the 425.94-nm line.

TABLE III. Experimental asymmetry data. Positions and amplitudes of the characteristic features of the antisymmetric deviation functions obtained from the measured line profiles. The deviation functions for the two similar plasma conditions were averaged since they vary only slightly. At the bottom of the table, averages and standard deviations are given for the positions of the minima, zero-crossing nodes, and maxima. These positions, given in units of the FWHM of the corresponding Lorentzian, are essentially constant and agree quite well with those obtained for the calculated line profiles (see Table II and last line of this table). The last two columns of the table compare theoretical and measured values of the ion broadening parameter A, the latter being obtained by comparison with the data in Table II. Theoretical values are derived from the tables published by Griem (Ref. 1).

Transition	Wavelength (nm)	Positions as fractions of the FWHM			Amplitudes of min. and max. deviations		Ion broadening parameter A	
		Minimum	Node	Maximum	Min. (%)	Max. (%)	Expt.	Theory
$4s'[\frac{1}{2}]^{\circ}_{0}$-$5p[\frac{1}{2}]_{1}$	452.23	0.228	0.472	0.730	−2.24	2.40	0.113	
$4s'[\frac{1}{2}]^{\circ}_{1}$-$5p'[\frac{1}{2}]_{0}$	425.94	0.209	0.454	0.762	−2.26	2.06	0.114	0.106
$4s'[\frac{1}{2}]^{\circ}_{1}$-$5p[\frac{1}{2}]_{0}$	451.07	0.190	0.464	0.863	−2.91	2.77	0.151	0.118
$4s'[\frac{1}{2}]^{\circ}_{1}$-$5p[\frac{1}{2}]_{1}$	470.23	0.206	0.445	0.795	−2.64	2.16	0.135	
$4s'[\frac{1}{2}]^{\circ}_{1}$-$5p[\frac{3}{2}]_{1}$	459.61	0.237	0.426	0.792	−2.62	1.88	0.134	
$4s'[\frac{1}{2}]^{\circ}_{1}$-$5p[\frac{5}{2}]_{2}$	462.84	0.212	0.490	0.870	−2.29	2.55	0.116	
$4s[\frac{3}{2}]^{\circ}_{1}$-$5p[\frac{3}{2}]_{1}$	427.22	0.213	0.462	0.823	−2.60	2.31	0.133	0.086
$4s[\frac{3}{2}]^{\circ}_{1}$-$5p[\frac{5}{2}]_{2}$	430.01	0.202	0.451	0.795	−2.67	2.19	0.137	
$4s[\frac{3}{2}]^{\circ}_{2}$-$5p[\frac{3}{2}]_{2}$	415.86	0.193	0.468	0.743	−2.50	2.19	0.127	
Averages:		0.210	0.459	0.797				
Standard deviations:		±6%	±4%	±7%				
Calculated data ($A=0.125$)		0.186	0.441	0.880				

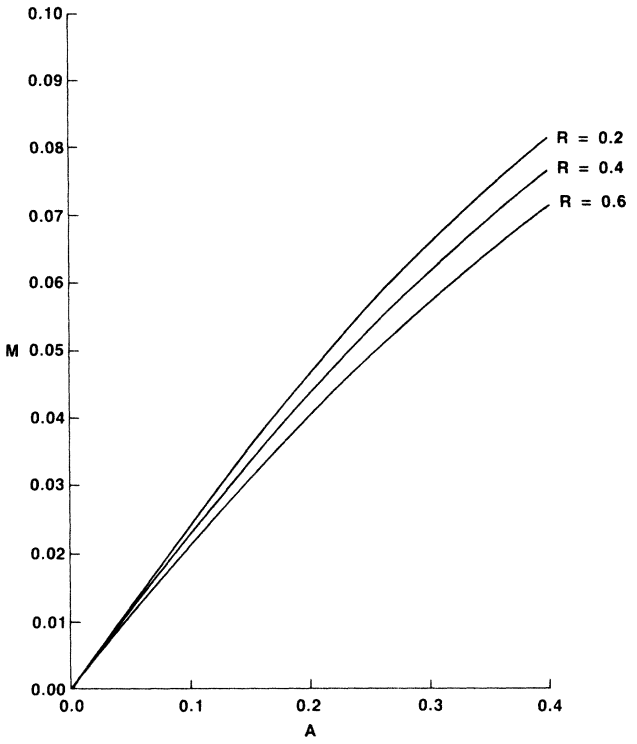

FIG. 3. Dependence of the amplitude M of the minimum of the calculated antisymmetric deviation functions (see Fig. 1) on the ion broadening parameter A for three values of the Debye screening parameter R.

For the general application of this new approach to determine, for red-shifted lines, the ion broadening parameter A from the amplitude of the minimum M of the antisymmetry function, it is useful to have a comprehensive plot of the calculated dependence of M versus A for the interesting range of A and R. We have generated such curves in Fig. 3 from the new profiles calculated by one of us (L.A.W.),[11] for the range $0.20 < R < 0.60$ which is the range encountered with low temperature plasma sources for which Stark broadening is significant. Curves are shown for only three different values of R, since the R dependence is so small that interpolations can be readily done. For this graph, we have not allowed for any continuum background in the theoretical profiles. (In our earlier analysis and comparisons, we had allowed—for reasons of consistency—for continuum backgrounds in both the experimental and calculated profiles.

VI. SUMMARY

In summary, the results of this study show that the quasistatic ion approximation in the Stark broadening theory of isolated lines of neutral atoms generates an accurate portrayal of ion broadened line profiles. The analysis of the deviations of both theoretical and measured line profiles from Lorentzian profiles serves as a useful technique for isolating the asymmetries in spectral line profiles that are due to ion broadening effects. Particularly, we have used the antisymmetric deviation functions generated from an analysis of theoretical line profiles to determine values of A to about a 10% accuracy. Since this technique relies on spectral-radiance measurements made near the line center, it has several advantages: (1) it utilizes radiance measurements made near line center where the signal-to-noise ratio is optimal, (2) the technique is relatively insensitive to the determination of the continuum background radiation which typically dominates the region of the far line wings, and (3) the technique makes it possible to measure ion broadening parameters for lines with other nearby lines that make line-wing measurements[12] impossible.

[1]H. R. Griem, *Spectral Line Broadening by Plasma* (Academic, New York, 1974).
[2]D. W. Jones and W. L. Wiese, Phys. Rev. A **30**, 2602 (1984).
[3]D. W. Jones and W. L. Wiese, Phys. Rev. A **29**, 2597 (1984).
[4]C. R. Vidal, J. Cooper, and E. W. Smith, Astrophys. J. Suppl. Ser. 214 **25**, 37 (1973).
[5]W. L. Wiese, in *Methods of Experimental Physics*, edited by B. Bederson and W. L. Fite (Academic, New York, 1968), Vol. 7B, pp. 307–353.
[6]H. R. Griem, M. Baranger, A. C. Kolb, and G. K. Oertel, Phys. Rev. **125**, 177 (1962).
[7]H. R. Griem, Phys. Rev. **128**, 515 (1962).
[8]C. F. Hooper, Jr., Phys. Rev. **165**, 215 (1968).
[9]W. L. Wiese, in *Plasma Diagnostic Techniques*, edited by R. H. Huddelstone and S. L. Leonard (Academic, New York, 1964).
[10]J. Barnard, J. Cooper, and E. W. Smith, J. Quant. Spectrosc. Radiat. Transfer **14**, 1025 (1974).
[11]L. Woltz, J. Quant. Spectrosc. Radiat. Transfer (to be published).
[12]O. Roder and A. Stampa, Z. Phys. **178**, 348 (1964).